NW9 (amino acid sequence after TEV cleavage)

GSTFSKLREQLGPVTQEFWDNLEKETEGLRQEMSKDLEEVKAKVQPYLDDFQKKWQEEMELYRQKVEPLGEEMRDRARAHVDALR
THLAPYSDELRQRLAARLEALKENGGARLAEYHAKATEHLSTLSEKAKPALEDLRQGLLPVLESFKVSFLSALEEYTKK**LNTQLPGT**G
AAALEHHHHHH

Peptide sequence

LNTQLPGTGSTFSK

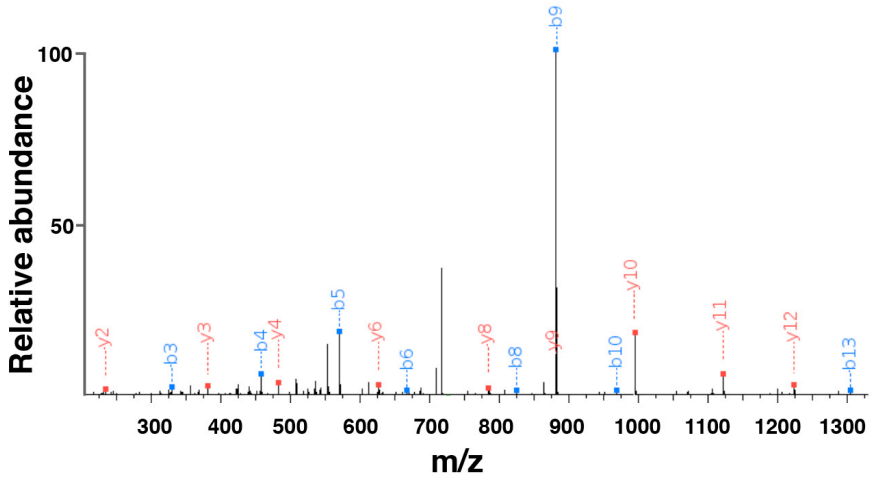

seq	#	b	y	#
L	1	114.091	---	14
N	2	228.134	1337.670	13
T	3	329.182	1223.627	12
Q	4	457.241	1122.579	11
L	5	570.325	994.520	10
P	6	667.377	881.436	9
G	7	724.399	784.384	8
T	8	825.446	727.362	7
G	9	882.468	626.314	6
S	10	969.500	569.293	5
T	11	1070.548	482.261	4
F	12	1217.616	381.213	3
S	13	1304.648	234.145	2
K	14	----	147.113	1

Supplementary Figure 1

Characterization of cNW9 by MS/MS confirms the ligation of the C terminus to the N terminus.

MS/MS spectrum of a tryptic fragment of cNW9 showing the ligation of the C-terminal motif (**LNTQLPGT**G-His_6) to the N-terminal residues (**GSTFSK**). Expected masses for b and y ions along with the peptide sequence are listed in the table. The b and y ions that were identified in the MS/MS spectrum are highlighted in blue and red. The full amino acid sequence of linear NW9 is shown at the top.

NW30 (amino acid sequence after TEV cleavage)

GSTFSKLREQLGPVTQEFWDNLEKETEGLRQEMSKDLEEVKAKVQPYLDDFQKKWQEEMELYRQKVEPLRAELQEGARQKLHELQ
EKLSPLGEEMRDRARAHVDALRTHLAPYSDELRQRLAARLEALKENGGARLAEYHAKATEHLSTLSEKAKPALEDLRQGLLPVLESFK
VSFLSALEEYTKKLNTQGTPVTQEFWDNLEKETEGLRQEMSKDLEEVKAKVQPYLDDFQKKWQEEMELYRQKVEPLRAELQEGAR
QKLHELQEKLSPLGEEMRDRARAHVDALRTHLAPYSDELRQRLAARLEALKENGGARLAEYHAKATEHLSTLSEKAKPALEDLRQGL
LPVLESFKVSFLSALEEYTKKLNTQGTPVTQEFWDNLEKETEGLRQEMSKDLEEVKAKVQPYLDDFQKKWQEEMELYRQKVEPLRA
ELQEGARQKLHELQEKLSPLGEEMRDRARAHVDALRTHLAPYSDELRQRLAARLEALKENGGARLAEYHAKATEHLSTLSEKAKPAL
EDLRQGLLPVLESFKVSFLSALEEYTKK**LNTQLPGT**GAAALEHHHHHH

Peptide sequence

LNTQLPGTGSTFSK

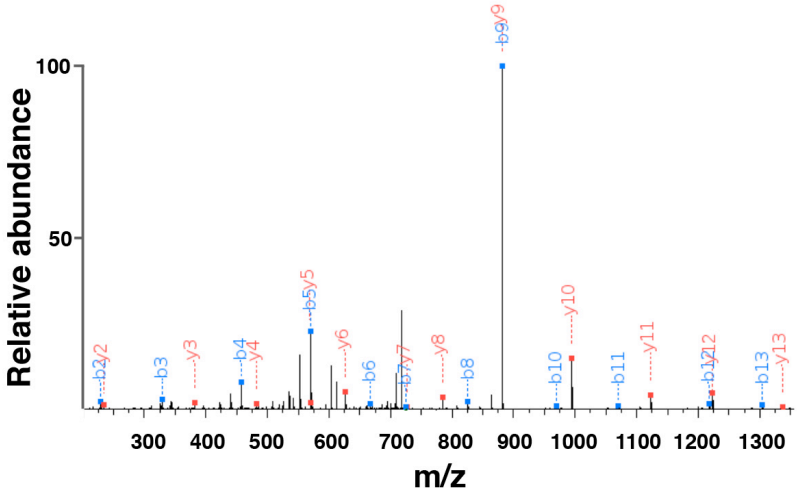

seq	#	b	y	#
L	1	114.091	---	14
N	2	228.134	1337.670	13
T	3	329.182	1223.627	12
Q	4	457.241	1122.579	11
L	5	570.325	994.520	10
P	6	667.377	881.436	9
G	7	724.399	784.384	8
T	8	825.446	727.362	7
G	9	882.468	626.314	6
S	10	969.500	569.293	5
T	11	1070.548	482.261	4
F	12	1217.616	381.213	3
S	13	1304.648	234.145	2
K	14	----	147.113	1

Supplementary Figure 2

Characterization of cNW30 by MS/MS confirms the ligation of the C terminus to the N terminus.

MS/MS spectrum of a tryptic fragment of cNW30 showing the ligation of the C-terminal motif (**LNTQLPGT**G-His_6) to the N-terminal residues (**GSTFSK**). Expected masses for b and y ions along with the peptide sequence are listed in the table. The b and y ions that were identified in the MS/MS spectrum are highlighted in blue and red. The full amino acid sequence of linear NW30 is shown at the top.

NW50 (amino acid sequence after TEV cleavage)

QGSTFSKLREQLGPVTQEFWDNLEKETEGLRQEMSKDLEEVKAKVQPYLDDFQKKWQEEMELYRQKVEPLRAELQEGARQKLHEL
QEKLSPLGEEMRDRARAHVDALRTHLAPYSDELRQRLAARLEALKENGGARLAEYHAKATEHLSTLSEKAKPALEDLRQGLLPVLES
FKVSFLSALEEYTKKLNTQGTPVTQEFWDNLEKETEGLRQEMSKDLEEVKAKVQPYLDDFQKKWQEEMELYRQKVEPLRAELQEGA
RQKLHELQEKLSPLGEEMRDRARAHVDALRTHLAPYSDELRQRLAARLEALKENGGARLAEYHAKATEHLSTLSEKAKPALEDLRQG
LLPVLESFKVSFLSALEEYTKKLNTQGTPVTQEFWDNLEKETEGLRQEMSKDLEEVKAKVQPYLDDFQKKWQEEMELYRQKVEPLR
AELQEGARQKLHELQEKLSPLGEEMRDRARAHVDALRTHLAPYSDELRQRLAARLEALKENGGARLAEYHAKATEHLSTLSEKAKPA
LEDLRQGLLPVLESFKVSFLSALEEYTKKLNTQGTPVTQEFWDNLEKETEGLRQEMSKDLEEVKAKVQPYLDDFQKKWQEEMELYR
QKVEPLRAELQEGARQKLHELQEKLSPLGEEMRDRARAHVDALRTHLAPYSDELRQRLAARLEALKENGGARLAEYHAKATEHLSTL
SEKAKPALEDLRQGLLPVLESFKVSFLSALEEYTKKLNTQGTPVTQEFWDNLEKETEGLRQEMSKDLEEVKAKVQPYLDDFQKKWQE
EMELYRQKVEPLRAELQEGARQKLHELQEKLSPLGEEMRDRARAHVDALRTHLAPYSDELRQRLAARLEALKENGGARLAEYHAKA
TEHLSTLSEKAKPALEDLRQGLLPVLESFKVSFLSALEEYTKK**LNTQLPGT**GAAALEHHHHHH

Peptide sequence
LNTQLPGTGSTFSK

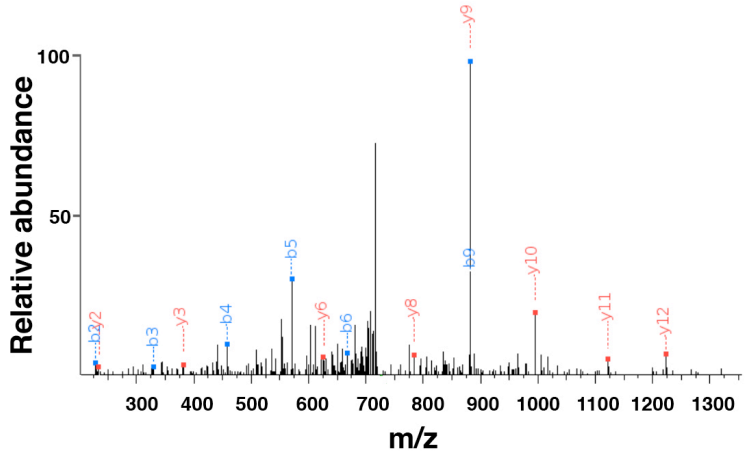

seq	#	b	y	#
L	1	114.091	---	14
N	2	228.134	1337.670	13
T	3	329.182	1223.627	12
Q	4	457.241	1122.579	11
L	5	570.325	994.520	10
P	6	667.377	881.436	9
G	7	724.399	784.384	8
T	8	825.446	727.362	7
G	9	882.468	626.314	6
S	10	969.500	569.293	5
T	11	1070.548	482.261	4
F	12	1217.616	381.213	3
S	13	1304.648	234.145	2
K	14	----	147.113	1

Supplementary Figure 3

Characterization of cNW50 by MS/MS confirms the ligation of the C terminus to the N terminus.

Spectrum of a tryptic fragment of cNW50 showing the ligation of the C-terminal motif (**LNTQLPGT**G-His_6) to the N-terminal residues (**GSTFSK**). Expected masses for b and y ions along with the peptide sequence are listed in the table. The b and y ions that were positively identified in the MS/MS spectrum are highlighted in blue and red. The amino acid sequence of linear NW50 (after TEV cleavage) is shown at the top.

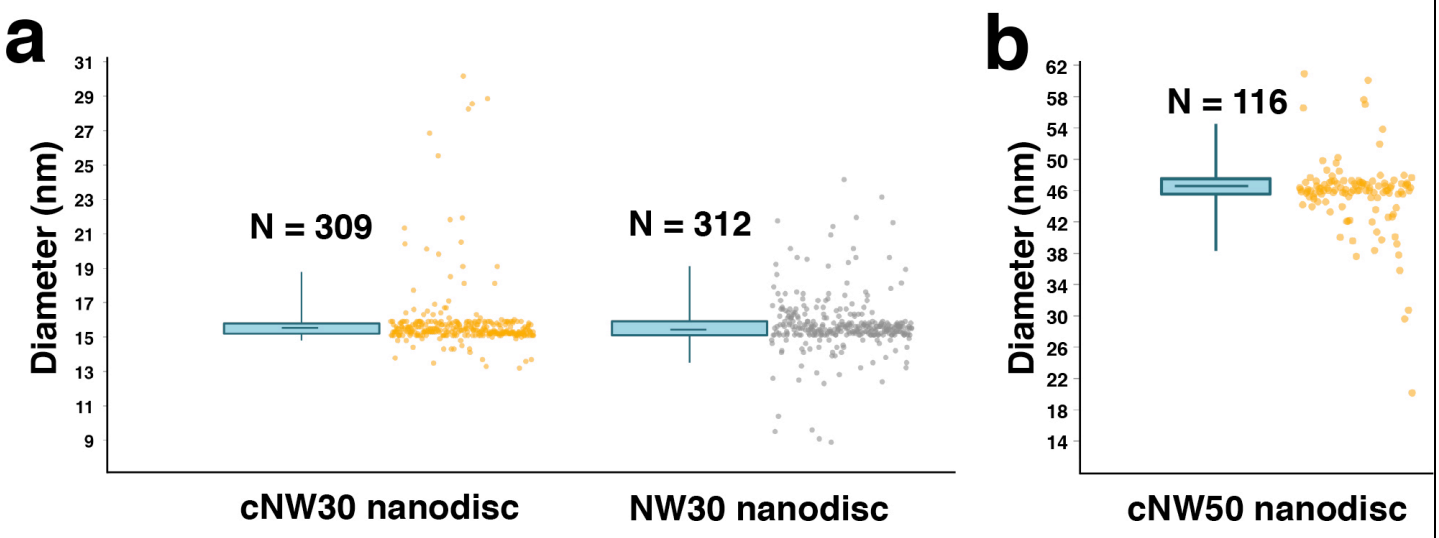

Supplementary Figure 4

Diameter distribution for nanodiscs assembled using cNW30, NW30 and cNW50 proteins.

(**a**) Diameter distribution for nanodiscs assembled using cNW30 (left) and NW30 (right). There is less variance in the lengths of cNW30 nanodiscs compared to NW30 nanodiscs (p=0.002). (**b**) Diameter distribution for nanodiscs made using cNW50. In the box-and-whisker plots, center lines show the means; box limits indicate the 25th and 75th percentiles; whiskers extend to the 5th and 95th percentiles. Raw data (jittered along x for clarity) are shown next to its representative plot. There is less variance in the lengths of cNW30 compared to NW30 nanodiscs (p = 0.002). Measurements were performed with the ImageJ software[29].

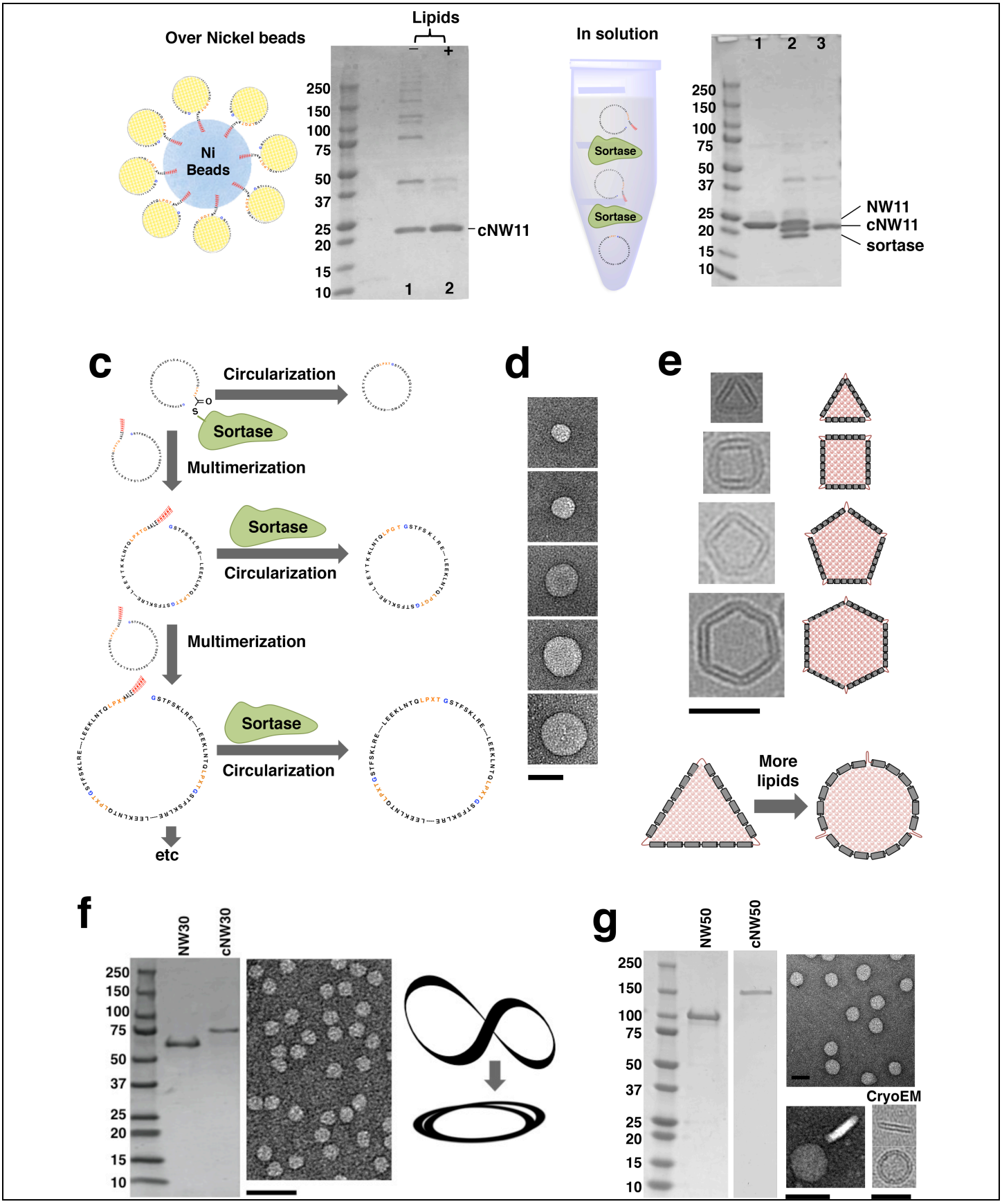
Over Nickel beads
Ni Beads
Lipids
–
+
250
150
100
75
50
37
25
20
15
10
cNW11
1
2
In solution
Sortase
Sortase
1
2
3
NW11
cNW11
sortase
c
Circularization
Sortase
Multimerization
Sortase
Circularization
Multimerization
Sortase
Circularization
etc
d
e
More lipids
f
NW30
cNW30
g
NW50
cNW50
CryoEM

Supplementary Figure 5

Producing covalently circularized nanodiscs with defined sizes and shapes.

(**a**) SDS-PAGE gel showing the final products after circularization over Ni beads with or without lipids. (**b**) Adding evolved sortase to diluted NW11 solution results mainly in NW11 circularization. Sortase was added to a dilute NW11 solution ([NW11] < 15 μM) to suppress linking two or more copies of NW11. (**c**) Adding evolved sortase to a concentrated NW11 solution leads to multimerization followed by circularization. (**d**) Negative-stain EM images showing large nanodiscs made using oligomeric circularized NW11. (**e**) Cryo-EM images of individual nanodiscs with different shapes. A triangle-shaped nanodisc is made using 3 copies of NW11 covalently linked together and circularized. Adding more lipids can change the shape back to a circular disc. Right: potential molecular arrangements of NW11 molecules around the differently shaped nanodiscs. (**f**) SDS-PAGE analysis of NW30 before and after circularization. Circularized NW30 migrates slower than its linear form. Right: negative-stain EM analysis of the nanodiscs made using circularized NW30 (cNW30) shows the formation of ~15 nm nanodiscs. (**g**) SDS-PAGE analysis of NW50 before and after circularization. Uncropped images are shown in **Supplementary note 2**. Right: negative-stain EM analysis of the nanodiscs made using circularized NW50 (cNW50) shows the formation of ~50 nm nanodiscs. Bottom: Negative-stain (left) and cryo-EM images (right) for individual nanodiscs showing top and side views. Scale bar, 50 nm.

NW30 and NW50 are sortaggable variants that we designed to assemble ~ 30- and 50-nm nanodiscs, respectively. Surprisingly, the cNW30 forms very homogenous ~15 nm instead of 30 nm nanodiscs On the other hand, as predicted, circularized NW50 assembled mainly ~ 50 nm nanodiscs.

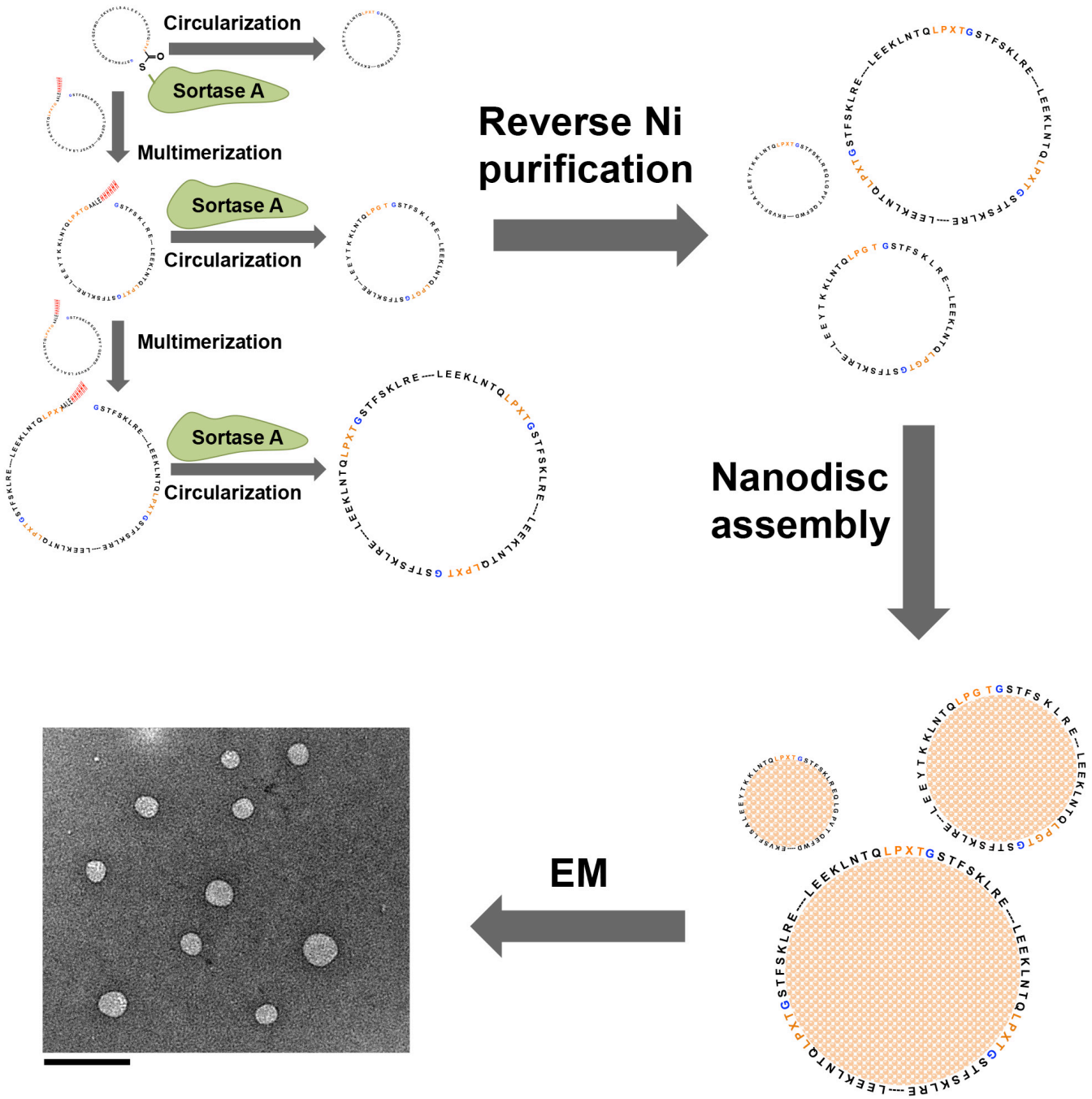

Supplementary Figure 6

The oligomeric, circularized species containing variable numbers of NW11 assemble into nanodiscs of various sizes.

Adding evolved sortase to concentrated NW11 solution leads to multimerization of NW11 followed by circularization. **Bottom**: Negative-stain EM image showing large nanodiscs made using oligomeric, circularized NW11. Scale bar, 100 nm.

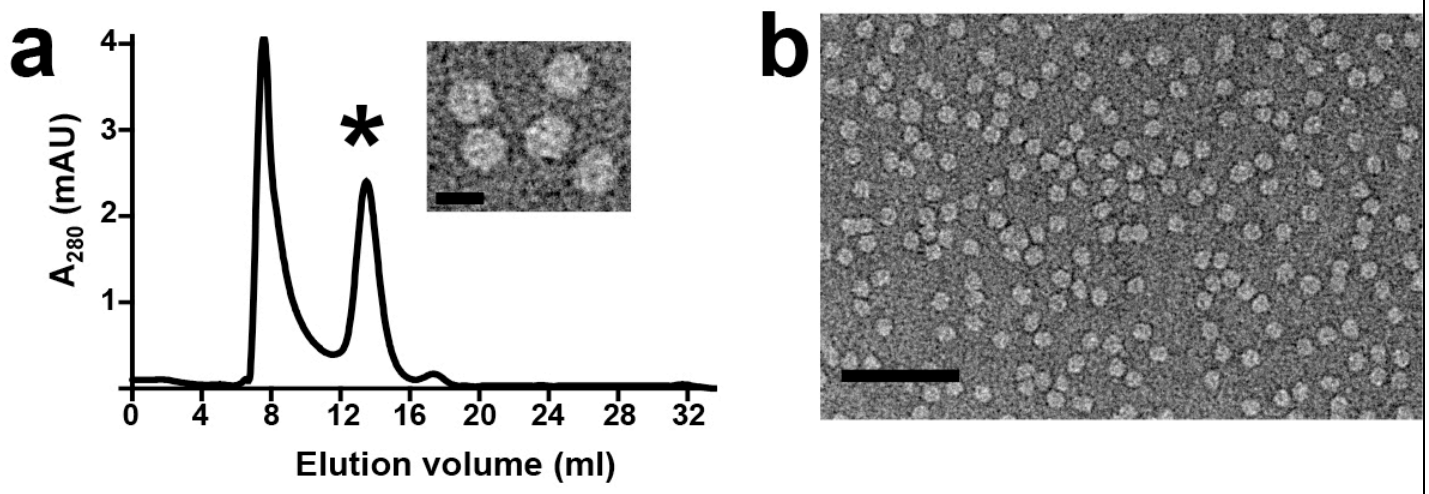

Supplementary Figure 7

Analysis of nanodiscs assembled using a cNW30:lipid ratio of 1:1000.

(**a**) Size-exclusion chromatography (SEC) analysis of the assembled nanodiscs. The SEC column (Superose 6 10/300) was equilibrated in 20 mM Tris-HCl, pH 7.5, 100 mM NaCl, 0.5 mM EDTA. The peak (labeled with *) was collected and analyzed by negative-stain EM (**b**). Scale bars, 15 nm (**a**) and 100 nm (**b**)

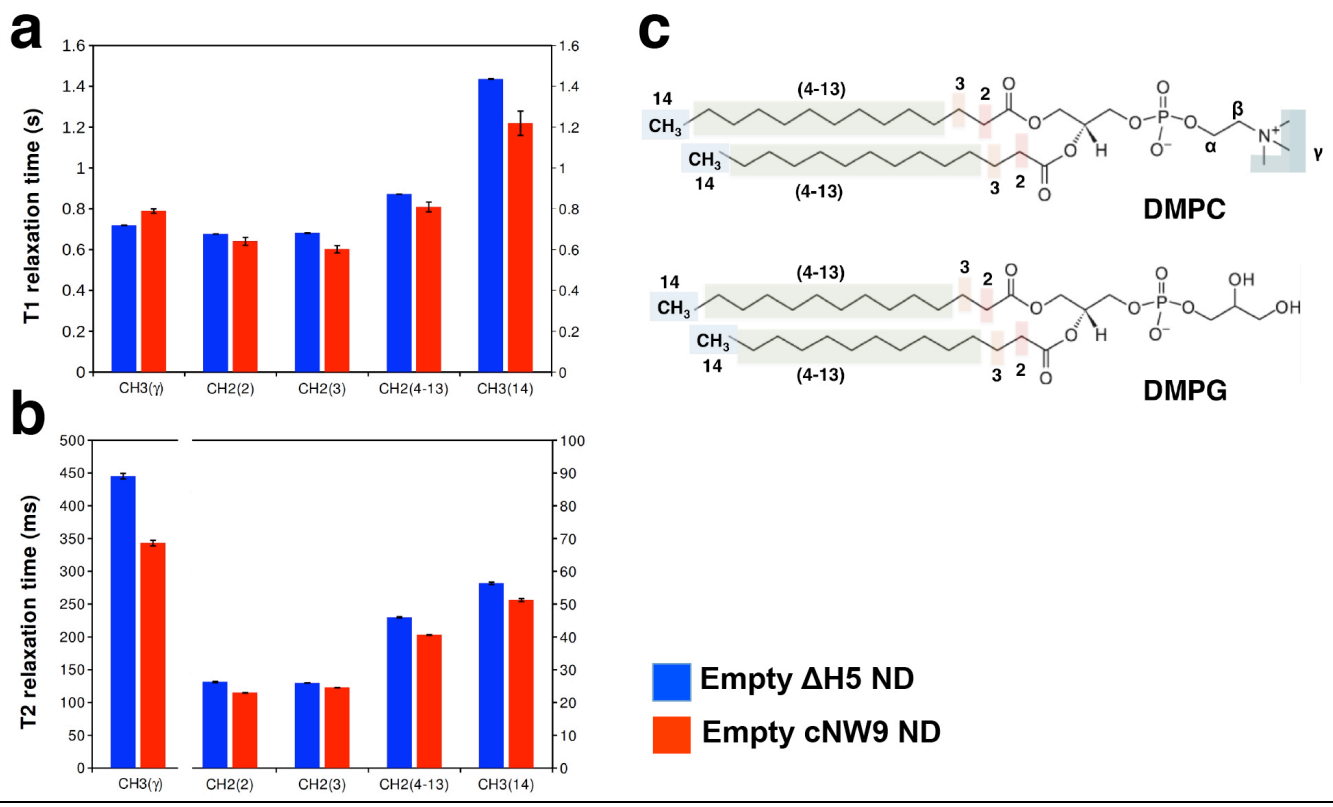

Supplementary Figure 8

Relaxation analysis of DMPC/DMPG (3:1) phospholipids in cNW and ΔH5 nanodiscs.

(**a**) ^{1}H-NMR T1 relaxation times of DMPC/DMPG lipid signals in empty ΔH5 (blue) and cNW9 (red) nanodiscs. (**b**) ^{1}H-NMR T2 relaxation times of DMPC/DMPG lipids signals in empty ΔH5 (blue) and cNW9 (red) nanodiscs (**c**) Chemical structure of DMPC and DMPG.

Except the DMPC γ methyl group located outside the bilayer region, the lipids in cNW9 show shorter T1 and T2 times consistent with smaller nanodisc size and dynamics indicative of the more restrictive circularized cNW9 belt. Measurements were acquired at 45ºC on a Bruker 500-MHz spectrometer using inversion recovery for T1 and CPMG refocusing train for T2.

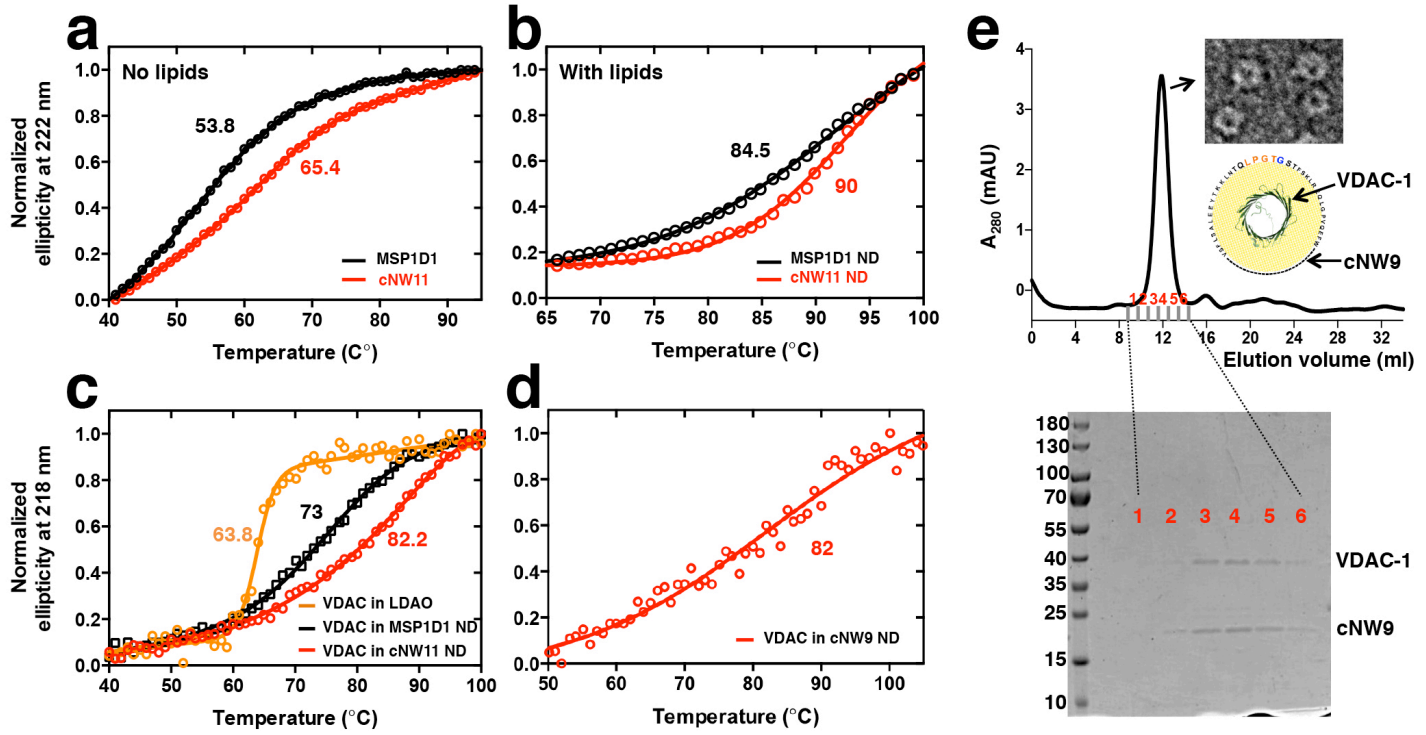

Supplementary Figure 9

Covalent circularization enhances thermal stability of MSPs and embedded VDAC-1.

Thermal unfolding of MSP1D1 (black) and cNW11 (red) without **(a)** and with lipids (**b**) followed by circular dichroism (CD) spectroscopy at 222 nm, the wavelength most characteristic of helical secondary structure. A lipid mixture of POPC:POPG at a molar ratio of 3:2 was used to generate nanodiscs. (**c**) Reconstitution into MSP1D1 nanodiscs increases the melting temperature, T_m, of VDAC1 by 9.2°C over that of VDAC1 in an LDAO micelle environment, and covalent circularization of the scaffold protein (cNW11) raises the T_m by an additional 9.2°C. Thermal unfolding of human VDAC-1 was followed by CD spectroscopy at 218 nm, the wavelength most characteristic of β-sheet secondary structure. Orange: VDAC1 in 0.1% LDAO, black: VDAC1 reconstituted into conventional nanodiscs (assembled using MSP1D1), and red: VDAC1 reconstituted into circularized nanodiscs (assembled using cNW11). Nanodiscs were made with a 3:2 POPC:POPG mixture. (**d**) Thermal unfolding of VDAC1 reconstituted into circularized nanodiscs (assembled using cNW9) followed by CD spectroscopy at 218 nm. Nanodiscs were made with POPC/POPG lipids at a molar ratio of 3:2. All samples were in 20 mM Tris-HCl, pH 7.5, 100 mM NaCl. **(e)** Analysis of the VDAC1 nanodisc assembly reaction. Top: size-exclusion chromatography and negative-stain EM of VDAC1 in cNW9 nanodiscs. The negative-stain EM shows nanodiscs containing a single channel. The stain-filled channels appear as dark spots inside the nanodiscs. Bottom: SDS-PAGE analysis of the nanodisc assembly. Fractions 1-6 were collected and analyzed.

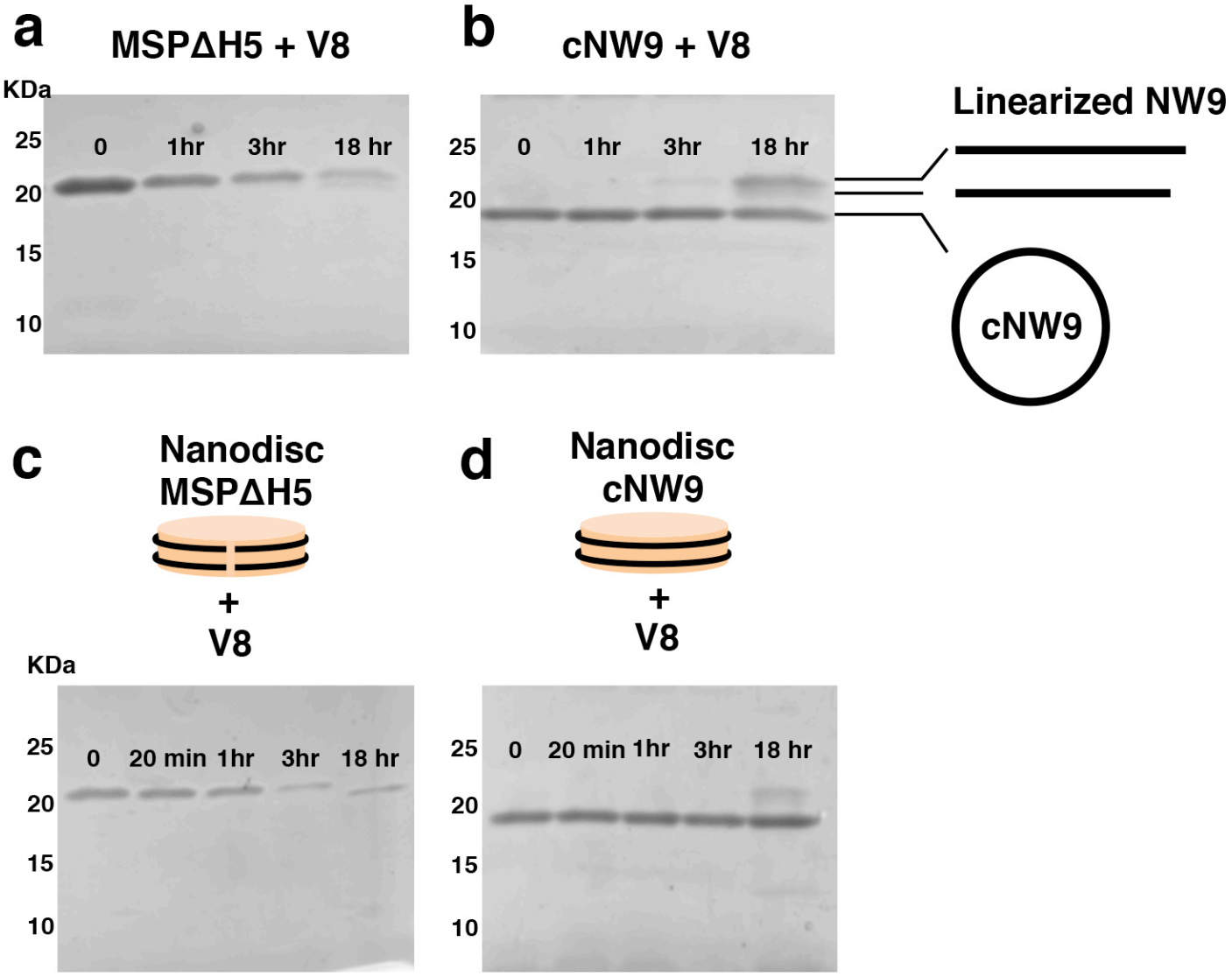

Supplementary Figure 10

Covalent circularization stabilizes MSPs against digestion by V8 protease without and with lipids.

(**a, b**) SDS-PAGE analysis of the proteolysis of lipid-free MSPΔH5 and cNW9. Samples were treated with V8 protease for 0 min (before addition of V8), and for 1, 3 and 18 hours. Lanes are labeled with times of protease treatment. Proteolysis was performed in 20 mM Tris-HCl, pH 7.5, 100 mM NaCl at 37°C and using a protein:protease ratio (w/w) of 1000:1. Treatment of MSPΔH5 with V8 resulted in the appearance of a large peptide, which is close in size to MSPΔH5 and is not discernible until about 18 hours after addition of V8; this peptide may be generated earlier but is not visible due to the low amount or overlap with uncleaved MSPΔH5. The intensity of the MSPΔH5 band decreased by 75% after 3 hours and by 93% after 18 hours. On the other hand, the intensity of the cNW9 band decreased by only 20% after 18 hours. A band that corresponds to linearized NW9 was observed after 3 hours and increased in intensity after 18 hours. (**c, d**) SDS-PAGE analysis of the proteolysis of nanodiscs assembled with MSPΔH5 and cNW9. Samples were treated with V8 protease for 0 min (before addition of V8), and for 20 min, 1, 3 and 18 hours. Proteolysis was performed at 37°C at pH 7.5 in 20 mM Tris-HCl, 100 mM NaCl using a 100:1 protein:protease (w/w). The band intensity of MSPΔH5 decreased by 81% after 3 hours. There was no decrease in the cNW9 band intensity up to 3 hours. The ImageJ software was used for analyzing band intensities.

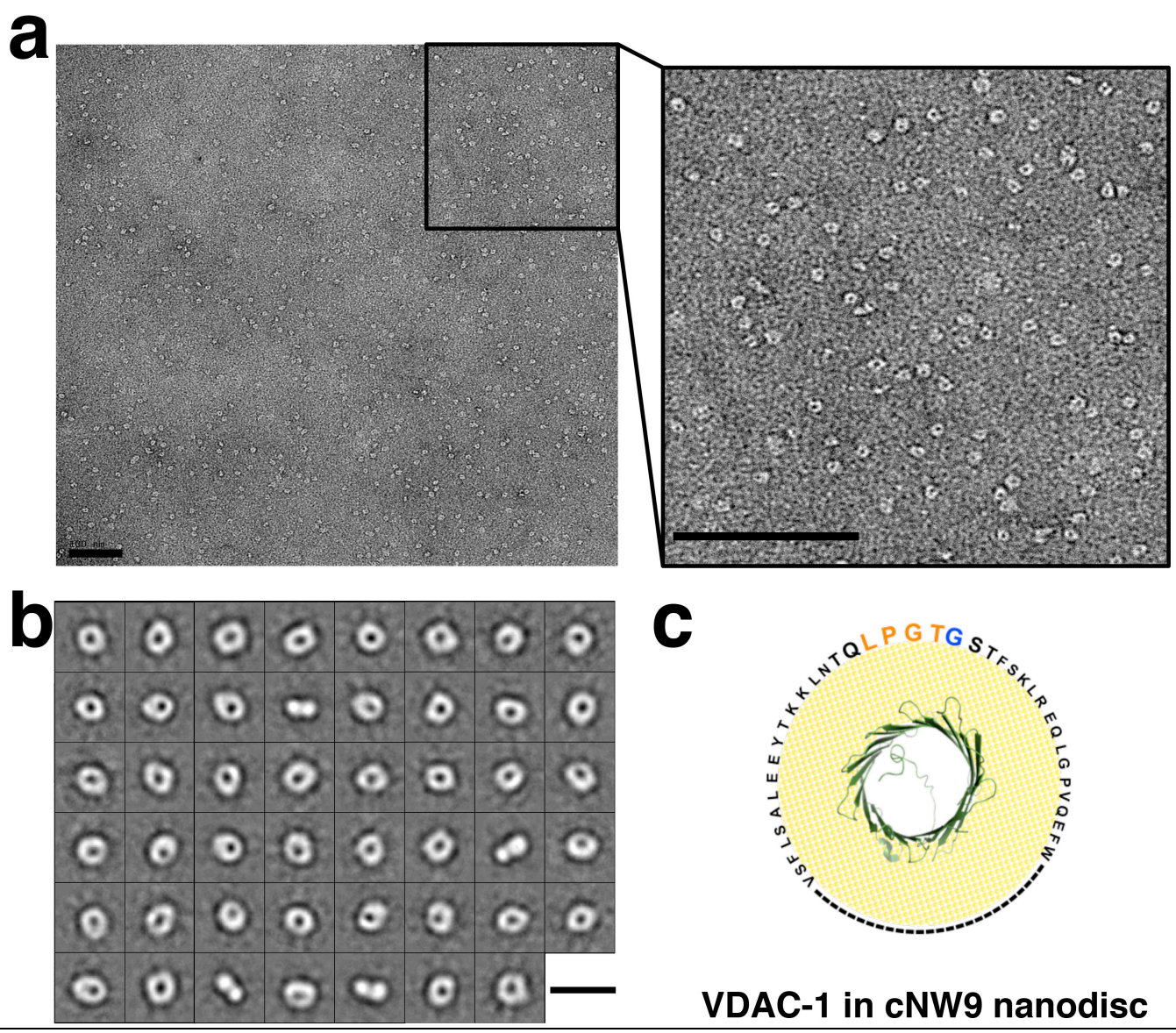

Supplementary Figure 11

Single-particle EM analysis of negatively stained VDAC-1 in cNW9 nanodiscs.

(**a**) Representative EM image of VDAC-1 in cNW9. Right. Enlarged image of the rectangular area in panel a, showing one VDAC-1 channel per nanodisc. Images were collected on a Tecnai T12 electron microscope (FEI) operated at 120 kV. (**b**) Representative two-dimensional (2D) class averages of VDAC-1 in cNW9 nanodisc, showing distinct views (top, tilted and side views). (**c**) Cartoon representation of VDAC-1 in a cNW9 nanodisc. Scale bars, 100 nm (**a**) and 20 nm (**b**)

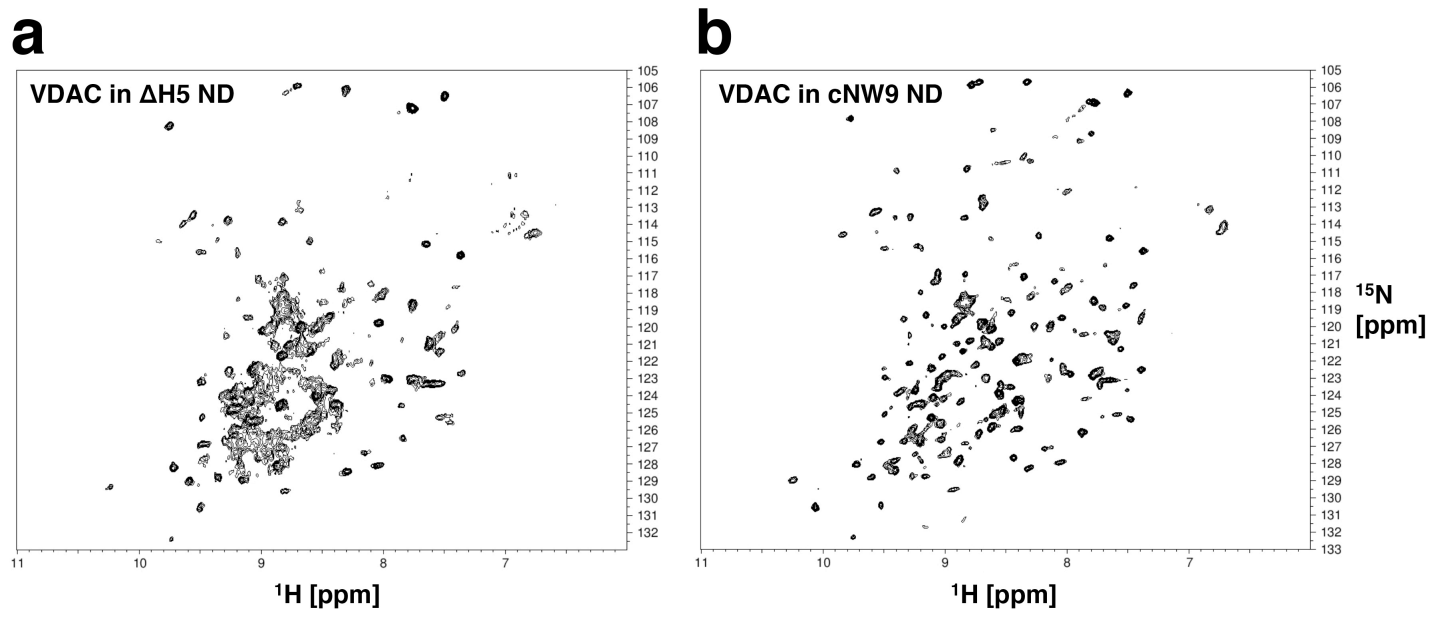

Supplementary Figure 12

Comparison of the quality of NMR spectra of VDAC-1 in ΔH5 and cNW9 nanodiscs.

(**a**) ^{1}H-^{15}N TROSY HSQC recorded at 45°C of 100 uM ^{15}N-^{2}D-labeled VDAC-1 in ΔH5 3:1 DMPC:DMPG nanodiscs acquired overnight on a 600-MHz spectrometer. (**b**) ^{1}H-^{15}N TROSY HSQC recorded at 45°C of 100 µM ^{15}N-^{2}D-labeled VDAC1 in cNW9 3:1 DMPC:DMPG nanodiscs acquired overnight on a 800-MHz spectrometer. The spectral quality and sample stability are greatly improved by using cNW9 as compared to ΔH5 nanodiscs.

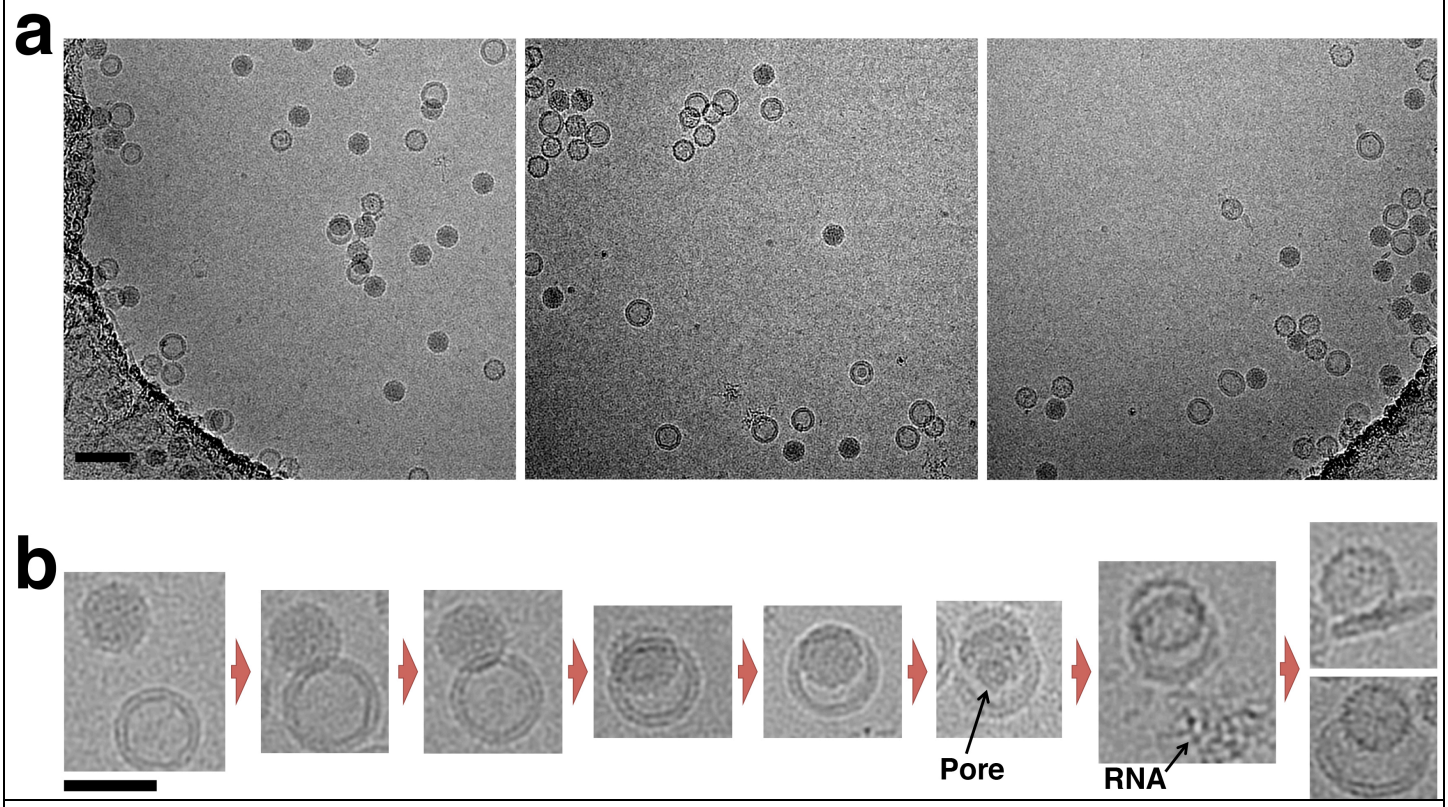

Supplementary Figure 13

Cryo-EM images of poliovirus plus CD155-decorated 50-nm nanodiscs.

(**a**) Representative cryo-EM images of poliovirus plus CD155-decorated 50-nm nanodiscs in vitreous ice. Scale bar represents 100 nm. (**b**) Representative cryo-EM images of poliovirus-nanodisc complexes showing different intermediate states. Scale bars, 100 nm (**a**) and 50 nm (**b**).

We find it unlikely that the putative pore in the nanodisc is a hexametric arrangement of CD155 since we used only the ectodomains of the receptor linked to lipid molecules via His tags. Scale bars, 100 nm (**a**) and 50 nm (**b**)

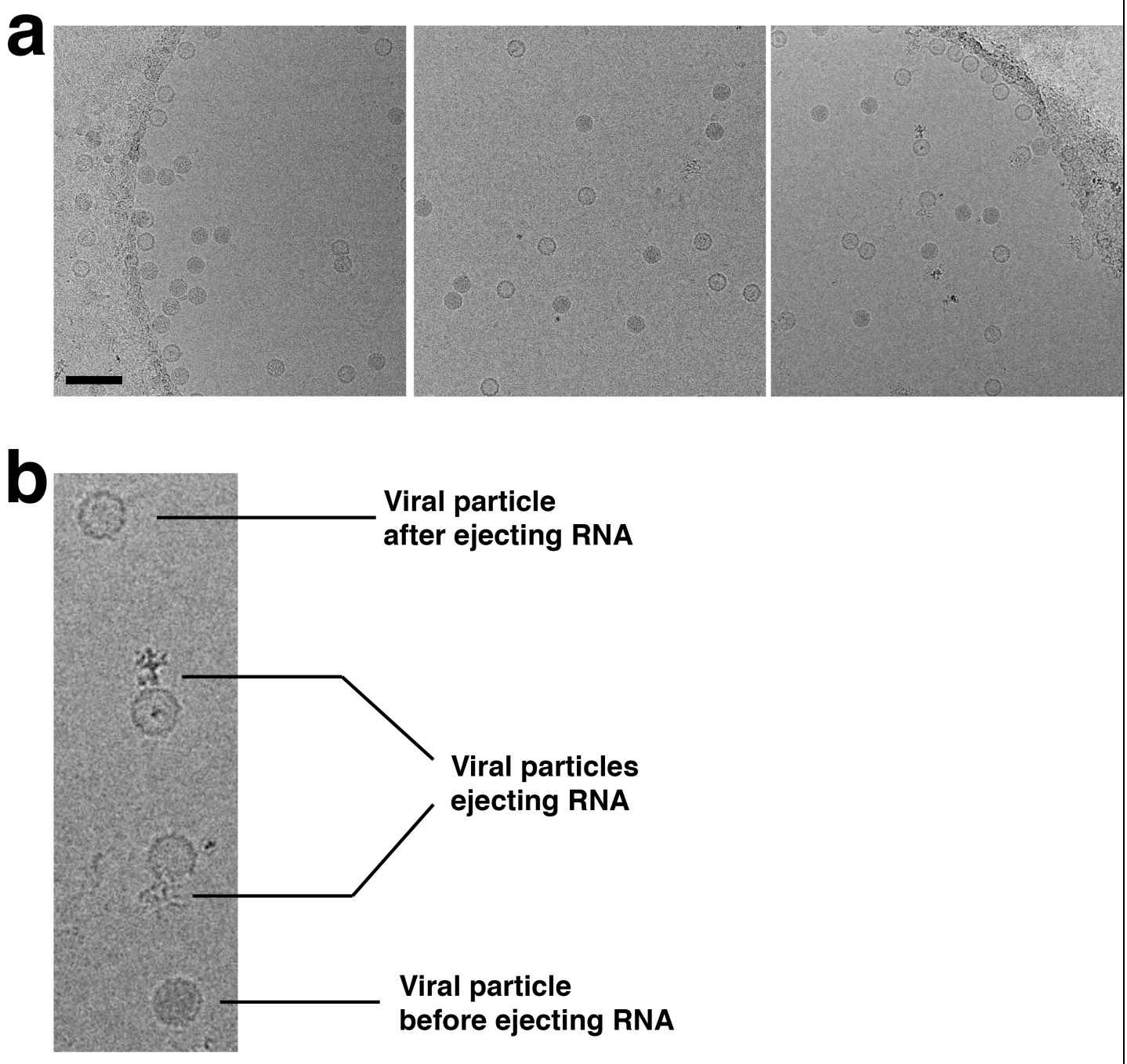

Supplementary Figure 14

Cryo-EM images of poliovirus plus CD155-decorated 15-nm nanodiscs.

(a) Representative cryo-EM images of poliovirus plus CD155-decorated 15-nm nanodiscs in vitreous ice. Scale bar represents 100 nm. **(b)** Cryo-EM image showing individual viruses ejecting RNA after incubation with CD155-decorated 15-nm nanodiscs. Scale bar, 100 nm.